Photon Control of Liquid Motion on Reversibly Photoresponsive Surfaces

Dongqing Yang,[†] Marcin Piech,[‡] Nelson S. Bell,[‡] Devens Gust,[§] Sean Vail,[§] Antonio A. Garcia,[⊥] John Schneider,[⊥] Choong-Do Park,[§] Mark A. Hayes,[§] and S. T. Picraux*,[†,#]

School of Materials, Department of Chemistry and Biochemistry, and Harrington Department of Bioengineering, Arizona State University, Tempe, Arizona, 85287, Sandia National Laboratories, Albuquerque, New Mexico, 87185, and Center for Integrated Nanotechnologies, Los Alamos National Laboratory, Los Alamos, New Mexico 87545

Received May 23, 2007. In Final Form: July 24, 2007

The movement of a liquid droplet on a flat surface functionalized with a photochromic azobenzene may be driven by the irradiation of spatially distinct areas of the drop with different UV and visible light fluxes to create a gradient in the surface tension. In order to better understand and control this phenomenon, we have measured the wetting characteristics of these surfaces for a variety of liquids after UV and visible light irradiation. The results are used to approximate the components of the azobenzene surface energy under UV and visible light using the van Oss−Chaudhury−Good equation. These components, in combination with liquid parameters, allow one to estimate the strength of the surface interaction as given by the advancing contact angle for various liquids. The azobenzene monolayers were formed on smooth air-oxidized Si surfaces through 3-aminopropylmethyldiethoxysilane linkages. The experimental advancing and receding contact angles were determined following azobenzene photoisomerization under visible and ultraviolet (UV) light. Reversible light-induced advancing contact-angle changes ranging from 8 to 16° were observed. A large reversible change in contact angle by photoswitching of 12.4° was achieved for water. The millimeter-scale transport of 5 μL droplets of certain liquids was achieved by creating a spatial gradient in visible/UV light across the droplets. A criterion for light-induced motion of droplets is shown to be consistent with the response of a variety of liquids. The type of light-driven fluid movement observed could have applications in microfluidic devices.

Introduction

Microfluidic systems are of interest for a variety of potential applications, such as delivering analyses in lab-on-chip environments, bioassays in drug discovery, and chemical analyses.[1−4] These applications are driving interest in handling increasingly smaller volumes of liquids in order to transport, store, mix, react, and analyze small amounts of liquids in miniaturized analytical systems. Benefits include reducing sample size, decreasing assay time, and minimizing reagent volume. However the physics of scaling does not permit a simple miniaturization of macroscopic pumps for liquid transport because of the increasing importance of interfacial forces relative to inertial forces as the surface-to-volume ratio increases. Thus, alternative methods to control the motion of small liquid volumes that scale favorably with decreasing liquid sample size are needed.

Some of the most promising new methods for manipulating liquid droplets on surfaces involve changing the interfacial properties of materials to control surface wetting by liquids. The key concept of these methods is that a gradient in surface tension can generate a net force for manipulation of the droplet on a surface. Such nonmechanically induced flow arising from the action of a surface tension gradient can be created by thermal,[5−7] electrochemical,[8−10] and chemical[11] methods. The use of light as a driving force offers unique opportunities.[12−17] Advantages anticipated for microfluidic systems driven by light include (i) the technology is amenable to miniaturization; (ii) no mechanical moving parts are needed; (iii) the use of light does not require contact of any additional materials with sensitive biological solutions; and (iv) chemical reactions can be performed on a tiny scale without the need for containers or channels.

Azobenzene is a well-known photochromic organic molecule that can be easily and reversibly photoisomerized from the trans to the cis form by UV irradiation, and from cis to trans by visible

* To whom correspondence should be addressed. E-mail: picraux@lanl.gov.
[†] School of Materials, Arizona State University.
[§] Department of Chemistry and Biochemistry, Arizona State University.
[⊥] Harrington Department of Bioengineering, Arizona State University.
[‡] Sandia National Laboratories.
[#] Los Alamos National Laboratory.

(1) Yager, P.; Weigl, B. H. *Science* **1999**, *283*, 346.
(2) Hayes, M. A.; Polson, N. A.; Phayre, A. N.; Garcia, A. A. *Anal. Chem.* **2001**, *73*, 5896.
(3) Bernard, A.; Michel, B.; Delamarche, E. *Anal. Chem.* **2001**, *73*, 8.
(4) Santini, J. T.; Cima, M. J.; Langer, R. *Nature* **1999**, *397*, 335.
(5) Liang, L.; Feng, X.; Liu, J.; Rieke, P. C. *J. Appl. Polym. Sci*. **1999**, *72*, 1.
(6) Sindy, K.; Tang, Y.; Mayers, B. T.; Vezenov, D. V.; Whitesides, G. M. *Appl. Phys. Lett*. **2006**, *88*, 061112.
(7) Paik, P.; Pamula, V. K.; Chakrabarty, K. *2004 Inter Society Conference on Thermal Phenomena*; IEEE: Los Alamitos, CA, 2004; pp 649−654.
(8) Whitesides, G. M.; Laibinis, P. E. *Langmuir* **1990**, *6*, 87.
(9) Gallardo, B. S.; Hwa, M. J.; Abbott, N. L. *Langmuir* **1995**, *11*, 4209.
(10) Gallardo, B. S.; Gupta, V. K.; Eagerton, F. D.; Jong, L. I.; Craig, V. S.; Shah, R. R.; Abbott, N. L. *Science* **1999**, *283*, 57.
(11) Chaudhury, M. K.; Whitesides, G. M. *Science* **1992**, *256*, 1539.
(12) Rosario, R.; Gust, D.; Hayes, M.; Jahnke, F.; Springer, J.; Garcia, A. A. *Langmuir* **2002**, *18*, 8062.
(13) Rosario, R.; Gust, D.; Garcia, A. A; Hayes, M.; Taraci, J. L.; Clement, T.; Dailey, J. W.; Picraux, S. T. *J. Phys. Chem. B* **2004**, *108*, 12640.
(14) Bunker, B. C.; Kim, B. I.; Houston, J. E.; Rosario, R.; Garcia, A. A.; Hayes, M.; Gust, D.; Picraux, S. T. *Nano Lett.* **2003**, *12*, 1723.
(15) Garcia, A. A.; Cherian, S.; Park, J.; Gust, D.; Jahnke, F.; Rosario, R. *J. Phys. Chem. A* **2000**, *104*, 6104.
(16) Rosario, R.; Gust, D.; Hayes, M.; Springer,J.; Garcia, A. A. *Langmuir* **2003**, *19*, 8801.
(17) Berna, J.; Leigh, D. A.; Lubomska, M.; Mendoza, S. M.; Perez, E. M.; Rudolf, P.; Teobaldi, G.; Zerbetto, F. *Nature* **2005**, *4*, 704.

10.1021/la701507r CCC: $37.00
Published on Web 09/06/2007

light. A solid surface modified with a photochromic azobenzene is a promising system for the control of surface free energy with light.[18−19] The photoinduced geometry change of azobenzene between trans and cis isomers results in a change in the molecular shape and dipole moment, which in turn gives rise to reversible switching of surface wettability through intermolecular interactions.[20−21] Thus, the reversible switching behavior of azobenzene upon exposure to light allows for optical control of surface wetting properties, and thereby control over fluid motion.

In this paper, we describe the photoinduced wetting/dewetting of azobenzene-functionalized surfaces for various liquids. This work follows our earlier studies of photoinduced movement of water drops on photochromic surfaces[13] and the light-driven liquid motion studies by Ichimura and colleagues[18−19] who formed photoresponsive azobenzene surfaces using *O*-octacarboxymethylated calix[4]resorcinarene (H-CRA-CM) absorbed onto fused silica surfaces with pendent *p*-octylazobenzene units as the photoresponsive adsorbate. In the present work, the azobenzene was covalently bound to a smooth, air-oxidized Si surface through pretreatment with 3-aminopropylmethyldiethoxysilane (ADES) followed by the formation of an amide bond with an azobenzene carboxylic acid.

The focus of this study was to examine the role of chemistry on the surface−liquid interaction and the change in droplet contact angle following UV−visible light irradiation of the photochrome. First, we measured contact angles using a variety of liquids for the azobenzene surface in both the cis and trans forms. These data were used in conjunction with the van Oss−Chaudhury−Good equation to estimate the surface energy components of the two solid surface states. We then examined the criteria for photoinduced droplet movement,[11,19] which requires that the change in contact angle upon photoisomerization exceeds the contact-angle hysteresis. The results were used to predict whether photoinduced movement of liquid drops could be achieved for various liquids on the basis of their wetting characteristics. These predictions were then tested by determining which liquid drops could be moved experimentally with light over millimeter distances.

1. Experimental Section

Synthesis. The synthetic route for azobenzene-acyl chloride (**5**) used in this study is illustrated in Figure 1 and was carried out as follows:

*4-[4′-(Pentylphenyl)azo]phenol (**1**).* This compound was prepared according to the procedure previously described.[22] 4-Pentylaniline (20.2 g, 124 mmol) was dissolved in a mixture of concentrated hydrochloric acid (HCl) (30 mL) and distilled water (40 mL). Sodium nitrite (8.6 g, 125 mmol) in distilled water (25 mL) was added dropwise to the above solution at 0 °C. The resulting solution of diazonium salt was added slowly to a mixture of phenol (11.6 g, 123 mmol) and sodium carbonate (21.4 g, 258 mmol) in distilled water (75 mL) at 0 °C. Pure **1** was obtained in nearly 100% yield.

*Isopropyl 11-Bromoundecanoate (**2**).* This compound was prepared in a manner similar to that described for a related compound.[23] A sample of 11-bromoundecanoic acid (25 g, 94 mmol) was reacted with oxalyl chloride (18 g, 141 mmol) in dichloroethane (DCE) (150 mL) at 70 °C for 30 min under N_2. DCE and residual oxalyl chloride were distilled under reduced pressure. Dichloromethane (90 mL), triethylamine (10.1 g, 100 mmol), and a catalytic amount of *N*,*N*-dimethylaminopyridine were added to the solution. Anhydrous isopropanol (11.3 g, 190 mmol) was subsequently added to the mixture at 5 °C. The reaction was warmed to room temperature and allowed to react for an additional 30 min. The reaction mixture was extracted with 5−10% (wt/wt) aqueous HCl, and the liquid was removed under reduced pressure. Compound **2** was isolated in 99% yield. ^{1}H NMR ($CDCl_3$, 400 MHz) 1.15 (6H, d, −CH(*CH*$_3$)$_2$), 1.21 (10H, m, −CH$_2$−(*CH*$_2$)$_5$−CH$_2$−), 1.36 (2H, m, −CH$_2$−*CH*$_2$−CH$_2$−), 1.55 (2H, m, −CH$_2$−*CH*$_2$−CH$_2$−), 1.77 (2H, m, −CH$_2$−*CH*$_2$−CH$_2$-), 2.18 (2H, t, -*CH*$_2$−CO−), 3.33 (2H, t, Br−*CH*$_2$−CH$_2$−), 4.93 (1H, m, −O*CH*(CH$_3$)$_2$).

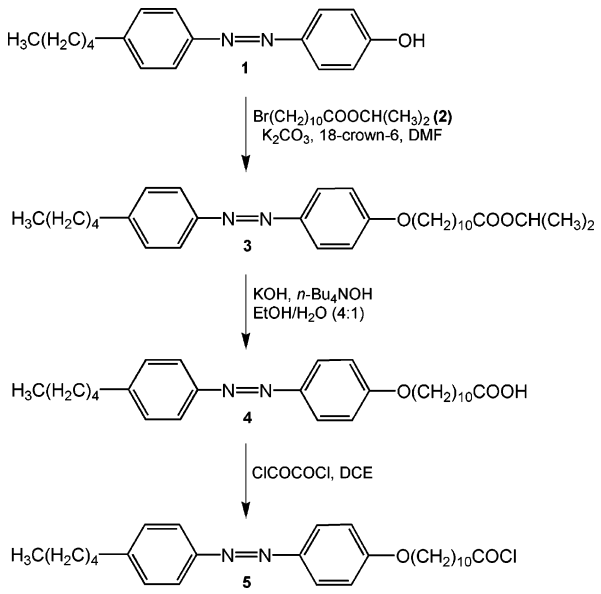

Figure 1. Synthetic route for azobenzene-acid chloride **5**.

*4-[(11-Isopropoxycarbonyl)undecyloxy]-4′-pentylazobenzene (**3**).* Isopropyl 11-bromoundecanoate **2** (14.4 g, 46.8 mmol), K_2CO_3 (8 g, 58 mmol), dicyclohexano-18-crown-6 catalyst (0.35 g, 1.0 mmol) and dimethylformamide (DMF) (100 mL) were combined in a 500 mL flask. A portion of **1** (12.6 g, 46.8 mmol) was then added, along with an additional 100 mL of DMF. The mixture was heated to 100 °C and allowed to react for 5 h under dry air. The liquid was removed by distillation under reduced pressure. After adding dichloromethane (200 mL) to the residue, the solution was washed with water (200 mL) and dried over Na_2SO_4. Volatiles were distilled under reduced pressure to leave pure product in 98% yield. ^{1}H NMR ($CDCl_3$, 400 MHz) 0.88 (3H, t, *CH*$_3$−CH$_2$−) 1.20 (6H, d, −CH-(*CH*$_3$)$_2$), 1.29 (14H, m, −CH$_2$−(*CH*$_2$)$_7$−CH$_2$−), 1.44 (2H, m, −CH$_2$−*CH*$_2$−CH$_2$−), 1.61 (4H, m, CH$_3$−(*CH*$_2$)$_2$−CH$_2$−), 1.79 (2H, m,−CH$_2$−*CH*$_2$−CH$_2$−), 2.24 (2H, t, −*CH*$_2$−CO−), 2.65 (2H, t, Ph−*CH*$_2$−), 4.01 (2H, t, Ph−O*CH*$_2$−), 4.98 (1H, m, -O*CH*(CH$_3$)$_2$), 6.97 (2H, d, Ph−*H*), 7.26 (2H, d, Ph−*H*), 7.78 (2H, d, Ph−*H*), 7.88 (2H, d, Ph−*H*).

*4-[(11-Carboxyundecyl)oxy]-4′-pentylazobenzene (**4**).* A portion of ester **3** (23 g, 46.4 mmol) was dispersed in 500 mL of 80/20 vol/vol ethanol/water solution. Potassium hydroxide (KOH) (22.5 g, 400 mmol) and 2 mL of 40 wt % aqueous tetra-*n*-butylammonium hydroxide (*n*-Bu$_4$NOH) were then added. The mixture was heated at reflux overnight, cooled to 0 °C, and acidified to pH 2 with 6 N hydrochloric acid. The aqueous layer was then extracted with dichloromethane and washed twice with 1 N HCl. Evaporation of the organic liquid under reduced pressure yielded 18 g of product (85.5% yield), which was used without further purification. ^{1}H NMR ($CDCl_3$, 400 MHz) 0.88 (3H, t, *CH*$_3$−CH$_2$−), 1.31 (14H, m, −CH$_2$−(*CH*$_2$)$_7$−CH$_2$−), 1.43 (2H, m, −CH$_2$−*CH*$_2$−CH$_2$−), 1.64 (4H, m, CH$_3$−(*CH*$_2$)$_2$−CH$_2$−), 1.79 (2H, m, −CH$_2$−*CH*$_2$−CH$_2$−), 2.33 (2H, t, −*CH*$_2$−COOH), 2.65 (2H, t, Ph−*CH*$_2$−), 4.01 (2H, t, Ph−O*CH*$_2$−), 6.97 (2H, d, Ph−*H*), 7.28 (2H, d, Ph−*H*), 7.77 (2H, d, Ph−*H*), 7.86 (2H, d, Ph−*H*).

*Azo-acid Chloride (**5**).* A portion of acid **4** (5 g, 11 mmol) was reacted with oxalyl chloride (2.9 g, 22.5 mmol) in DCE (250 mL)

(18) Oh, S. K.; Nakagawa, M.; Ichimura, K. *J. Mater. Chem.* **2002**, *12*, 2262.
(19) Ichimura, K.; Oh, S. K.; Nakagawa, M. *Science* **2000**, *288*, 1624.
(20) Siewierski, L. M.; Brittain, W. J.; Petrash, S.; Foster, M. D. *Langmuir* **1996**, *12*, 5838.
(21) Natansohn, A.; Rochon, P.; *Chem. Rev.* **2002**, *102*, 4139.
(22) Siewierski, L. M.; Lander, L. M.; Leibmann, A.; Brittain, W. J.; Foster, M. D. *SPIE Proc.* **1995**, *2441*, 1.
(23) Sekkat, A.; Wood, J.; Geerts, Y.; Knoll, W. *Langmuir* **1996**, *12*, 2976.

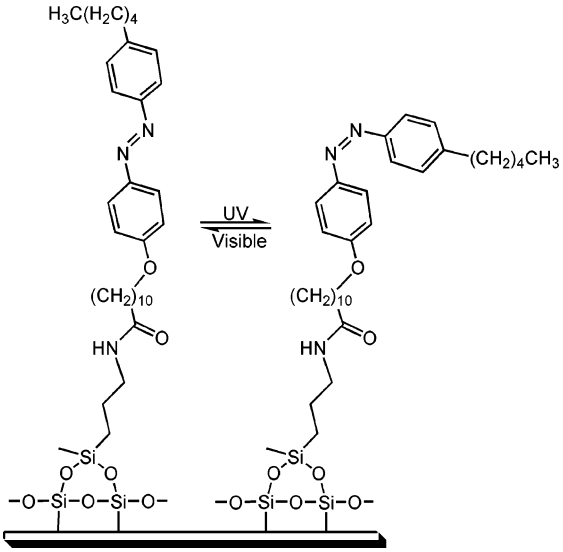

Figure 2. Molecular structure of azobenzene tethered to the surface via ADES, illustrating the trans and cis states after visible and UV irradiation, respectively.

at 70 °C for 1 h under N_2. The liquid and residual oxalyl chloride were removed by distillation to give pure product in 99% yield. ^{1}H NMR ($CDCl_3$, 400 MHz) 0.90 (3H, t, CH_3−CH_2−), 1.34 (14H, m, −CH_2−(CH_2)$_7$−CH_2−), 1.48 (2H, m, −CH_2−CH_2−CH_2−), 1.69 (4H, m, CH_3−(CH_2)$_2$−CH_2−), 1.82 (2H, m, −CH_2−CH_2−CH_2−), 2.67 (2H, t, Ph−CH_2−), 2.88 (2H, t, −CH_2−COCl), 4.04 (2H, t, Ph−OCH_2−), 6.96 (2H, d, Ph−*H*), 7.30 (2H, d, Ph−*H*), 7.80 (2H, d, Ph−*H*), 7.89 (2H, d, Ph−*H*). MALDI-MS (terthiophene matrix): calculated 470.27, found 471.25 [M + H].

Materials. Polished silicon (100) *n*-type 4 in. wafers were obtained from WaferNet, Inc., and their surfaces were confirmed to be quite smooth (atomic force microscopy gave root-mean-square (rms) roughnesses in the subnanometer range). The ADES was obtained from Gelest, Inc. Toluene was obtained from Mallinckrodt Baker, Inc. and was double distilled prior to use. Deionized (DI) water used for contact-angle measurements was obtained from a Barnstead Nanopure system. All probe liquids used for contact-angle measurements were obtained from Alfa Aesar or Aldrich and used as received.

Substrate Monolayer Functionalization. Si (100) *n*-type substrates with an air-oxidized surface were cut into rectangular samples of about 1.5 cm × 3 cm. These samples were cleaned with a UV ozone treatment (UV ozone cleaner, model 42, Jelight, Inc.) for 30 min, rinsed extensively with DI water, and dried in an oven at 140 °C for 15 min. After cleaning, the substrate was immersed in a solution of 100 μL ADES in 10 mL of double-distilled toluene for 30 min at room temperature, washed well three times in toluene to remove excess reagent, and heated in an oven at 140 °C for 3 h. The aminosilane-coated substrate was incubated in an oven at 80 °C in a toluene solution of **4** (20 mM) in the presence of 4-dimethylaminopyridine (200 mM) for 8 h. The substrate was then removed from solution, washed sequentially with toluene, dichloromethane, and tetrahydrofuran for 5 min, and dried with nitrogen gas. This treatment results in azobenzene tethered to the SiO_2 surface through a siloxane (ADES) as the linker molecule (ADES-AZO) as shown schematically in Figure 2. Glass substrates with tethered azobenzene were also prepared for UV−vis absorption studies. The glass slides were cleaned in a warm sulfuric acid and hydrogen peroxide (2:1) solution for 30 min, rinsed in DI water, and then cleaned in a warm hydrogen peroxide and hydrochloric acid solution (1:1) for 30 min and finally rinsed with DI water. After this cleaning treatment, the same procedure as that described above for functionalizing the azobenzene monolayer on the surface was used.

Physical Measurements. The UV−vis absorption spectrum of an ADES-AZO monolayer prepared on glass is presented in Figure 3. Although trans and cis azobenzene exhibit overlapping absorption,

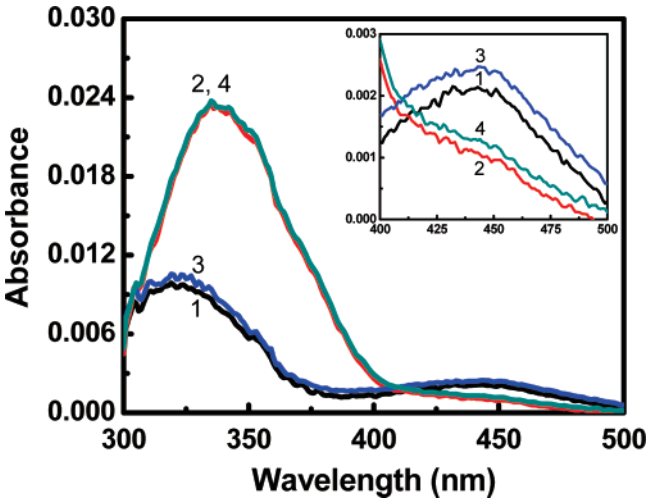

Figure 3. UV−visible absorbance spectra for an ADES-AZO surface under a sequence of visible and UV irradiation; inset shows the 445 nm peak region enlarged. Spectra were taken in the following order: curve 1 (black line) ADES-AZO surface exposed to UV light for 5 min; curve 2 (red line) after visible irradiation for 5 min; curve 3 (blue line) after a second UV irradiation for 5 min; curve 4 (green line) after visible irradiation for 10 min.

the two forms can be readily distinguished.[24] The photoirradiation of the ADES-AZO monolayer with UV (366 nm) light results in the formation of the cis isomer, with an absorption band at 445 nm. The prominent peak at 340 nm observed following exposure of the ADES-AZO monolayer to visible light is attributed to the $n\rightarrow\pi^*$ electronic transition for the trans isomer. Curves 1−4 in Figure 3 illustrate the change in the absorption bands during switching with various UV and visible light exposure times. These changes observed in the UV−vis absorption spectrum confirm the reversible photoisomerization of the ADES-AZO monolayer between cis and trans forms. Because both isomers absorb at both of the wavelengths used for irradiation, at equilibrium under either light the sample is present as a photostationary distribution of the two isomers, enriched in one form.

Contact-Angle Measurements. The dynamic contact-angle measurements were performed using a Ramé−Hart standard automated goniometer, model 200-00. This equipment included the DROP image standard software that uses a curve-fitting routine for contact-angle calculations. The dynamic advancing and receding contact angles were measured while gradually increasing and decreasing the volume of liquid with the dispensing needle embedded in the sessile drop. All measurements were carried out at room temperature. Figure 4 illustrates the contact-angle measurement method. The volume of the droplet is increased by adding liquid from t_0 to t_2 and decreased by removing liquid from t_2 to t_4. As the volume of the droplet is increased from t_0 to t_1, the contact angle (Figure 4, upper curve) is seen to increase, and the droplet maintains the same contact area with the surface. At t_1, the droplet begins to increase in surface contact area, and, as the volume of droplet increases from t_1 to t_2 (as indicated by the droplet width in Figure 4, middle curve), the area continues to advance over the unwetted area while keeping the same maximum contact angle. Thus, the advancing contact angle, θ_{adv}, is measured by averaging this maximum angle over a large number of measurements while increasing the liquid volume from t_1 to t_2. From t_2 to t_3, the volume of the droplet decreases, and the contact angle decreases while maintaining the same contact area. At t_3, the contact area begins to decrease with a constant minimum angle from t_3 to t_4 as the volume of liquid in the droplet is decreased. The receding contact angle, θ_{rec}, is obtained by averaging this minimum angle over a corresponding large number of measure-

(24) Zimmerman, G.; Chow, L-Y.; Paik, U-J. *J. Am. Chem. Soc.* **1958**, *80*, 3528.
(25) Wright, D.; Caldwell, R.; Moxely, C.; El-Shall, M. S. *J. Chem. Phys.* **1993**, *98*, 3356.

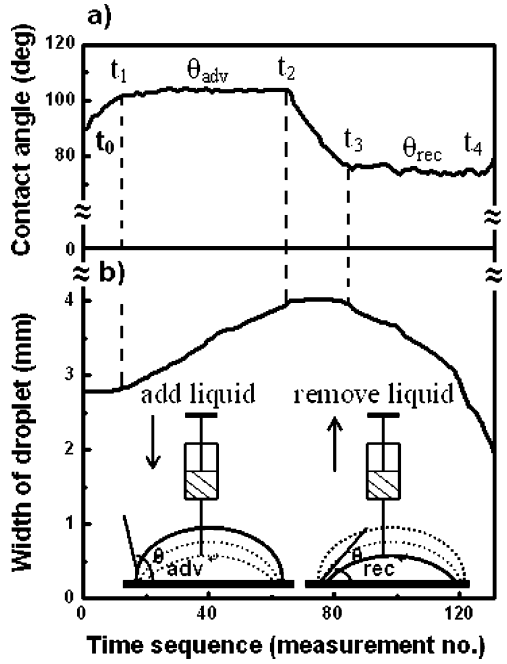

Figure 4. The dynamic advancing and receding contact-angle measurement method is illustrated for water, with the top curve (a) being a plot of the contact angle and the middle curve (b) being the width of the sessile drop. These values are continuously measured as a function of time while adding liquid (time t_0 to t_2) or removing liquid (time t_2 to t_4) from the drop. The advancing contact angle is determined by the average value between t_1 and t_2, where the contact angle has reached it maximum value and the contact area of the drop is continuously growing in size. The receding contact angle is given by the average value between t_3 and t_4, where the contact angle has reached its minimum value and the contact area of the drop is continuously decreasing in size.

ments between t_3 to t_4 as liquid is removed from the droplet. By averaging over an large number of measurements in this way and by repeating these measurements on multiple locations (typically five) on the azobenzene-functionalized surfaces for the dynamic advancing and receding contact angles for each liquid studied, the accuracy was improved over single contact-angle measurements at each location. The contact-angle hysteresis is defined as the difference between the above-measured dynamic advancing and receding contact angles.

Photoirradiation. The UV light source was a model UVGL-25 Mineralight lamp with 254 and 366 nm wavelengths. We used the 366 nm light for 5 min for the UV irradiations with a flux of 2 mW cm^{-2} at the sample surface. The visible light source was a model 190 Fiber optic illuminator from Dolan-Jenner Industries (Lawrence, MA), coupled with a 410 nm-long wave length pass filter, resulting in a flux of 10 mW cm^{-2} on the sample surface. An exposure time of 5 min was also used for the visible light irradiations.

2. Results and Discussion

Photoswitchable ADES-AZO Surface. We prepared azobenzene-functionalized monolayer surfaces on smooth air-oxidized Si substrates in order to use the photochromic property of azobenzene to reversibly switch between trans and cis states, thereby altering the surface energy. Under visible light, azobenzene is present mainly as the *trans* isomer, and the drops exhibit a higher contact angle; under UV light, azobenzene is present mainly as the cis isomer, and drops display a lower contact angle. Figure 5 shows reversible water wettability after visible and UV irradiation on the ADES-AZO surface. The water contact-angle changes from 100−102° under visible light to 88−89° under UV light. The reversible photoinduced advancing contact-angle change was therefore 11−13°. This observed contact-

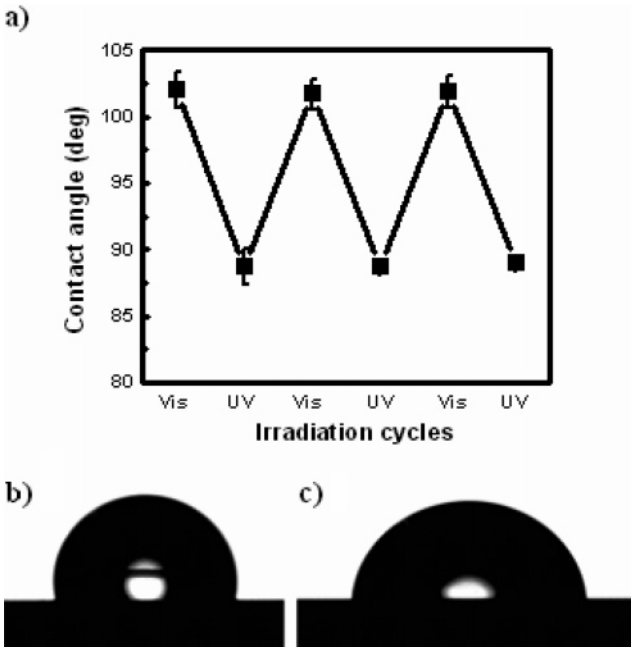

Figure 5. (a) Reversible advancing contact angle for water as measured on the ADES-AZO surface, showing reversible switching as a function of sequential visible and UV light irradiation. (b) Side-view photograph of the water droplet after irradiation with visible light. (c) Side view photograph of the water droplet after irradiation with UV light. A comparison of panels b and c illustrates the decrease in advancing contact angle with UV irradiation.

angle switching is approximately 50% greater than values noted in earlier studies. Oh et al. used an *O*-octacarboxymethylated calyx resorcinarene with pendent *p*-octylazobenzene units as a photoresponsive adsorbate (H-CRA-CM), and observed contact-angle switching of 8° using visible and UV illumination.[18] Siewierski and co-workers prepared monolayer assemblies on silicate substrates by direct deposition of alkyltriethoxysilanes followed by covalent attachment of azobenzene derivatives to the functionalized layers. Their contact-angle switching ranged from 4° to 9°.[20] The larger contact-angle switching values reported here suggest that the present method of tethering the azobenzene to the surface allows for greater interaction between the liquid and azobenzene moieties while maintaining sufficient free volume for photoisomerization.

Contact Angles of Different Liquids on ADES-AZO Surfaces. To investigate the dependence of liquid−solid interactions on liquid properties, we measured the advancing (θ_{adv}) and receding (θ_{rec}) contact angles for various liquids on the azobenzene-modified surface following both visible and UV (366 nm) irradiation. The liquids were diiodomethane, 1-bromonaphthalene, 1-methylnaphthalene, DMF, acetonitrile, benzonitrile, formamide, and ethylene glycol. We prepared two or three samples for each liquid and measured five different contact areas for each sample. Contact-angle results for each liquid after visible/UV irradiation of the surface are summarized in Table 1.

Surface Energy of Azobenzene. The contact angle on the azobenzene-modified surfaces increases approximately linearly with the surface tension of the probe liquids after both UV and visible irradiation, as shown in Figure 6. These trends suggest that results for the various probe liquids can provide insight into the energetics of the azobenzene−fluid interface and, consequently, the fluid transfer properties at this interface.

The surface free energy is an important parameter that plays a major role in a variety of interfacial physicochemical processes. Although there are several methods for estimating surface

Table 1. Contact Angles on an ADES-AZO Surface for Various Liquids[a]

liquid	contact angle change[b] $\Delta\theta_s$ (deg)	hysteresis[c] $\Delta\theta_h^{trans}$(deg)	surface tension (mN/m)	contact angle (deg): trans θ_{adv}	contact angle (deg): trans θ_{rec}	contact angle (deg): cis θ_{adv}	contact angle (deg): cis θ_{rec}
acetonitrile	15.5	7.6	28.7[d]	27.0	19.4	11.5	<5
benzonitrile	15.0	5.8	38.8[d]	32.0	26.2	17.0	<5
DI water	12.4	25.3	72.8[e]	101.3	76.0	88.9	69.8
diiodomethane	12.0	10.4	50.8[e]	54.1	43.7	42.1	33.1
DMF	10.7	7.9	36.8[f]	37.5	29.6	26.8	19
formamide	10.7	19.4	58.0[e]	82.2	62.8	71.5	58.2
1-methylnaphthalene	10.0	9.8	38.7[g]	33.3	23.5	23.3	13.5
ethylene glycol	9.3	24.2	48.0[e]	73.2	49.0	63.9	41.5
1-bromonaphthalene	8.3	4.5	44.4[e]	38.0	33.5	29.7	24.6

[a] The measured standard deviations are reported in Table 1 of the Supporting Information. [b] The light-induced contact-angle change, $\Delta\theta_s$, is defined as the difference between the advancing contact angles for visible irradiation minus that for UV irradiation: $\Delta\theta_s = \theta_{adv}^{trans} - \theta_{adv}^{cis}$. [c] The hysteresis for the trans state (after visible light irradiation), $\Delta\theta_h$, is given by $\Delta\theta_h^{trans} = \theta_{adv}^{trans} - \theta_{rec}^{trans}$. [d] Reference 25. [e] Reference 26. [f] Reference 27. [g] Reference 28.

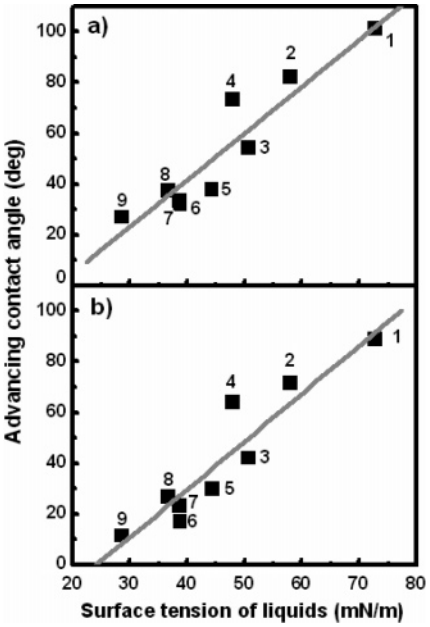

Figure 6. Advancing contact angle measured on the ADES-AZO surface vs surface tension for the various probe liquids studied after (a) visible and (b) UV light irradiation. The liquids as numbered in the plots are (1) DI water, (2) formamide, (3) diiodomethane, (4) ethylene glycol, (5) 1-bromonaphthalene, (6) benzonitrile, (7) 1-methylnaphthalene, (8) DMF, and (9) acetonitrile. Lines are linear best fits with slopes of 1.89°/mN/m for panel a and 1.93°/mN/m for panel b.

energies, the Lifshitz−van der Waals/acid−base (LWAB) approach suggested by van Oss and co-workers[26,27,29] is straightforward and has proven to be of fairly general applicability.[28,30] According to the van Oss theory, the surface free energy γ_S can be expressed by eq 1:

$$\gamma_S = \gamma_S^{LW} + \gamma_S^{AB} \quad (1)$$

$$\gamma_S^{AB} = 2\sqrt{\gamma_S^- \gamma_S^+} \quad (2)$$

Table 2. Probe Liquid Free-Energy Components (mJ/m^2) Used for Calculations[27]

liquids	γ_L	γ_L^{LW}	γ_L^-	γ_L^+	γ_L^{AB}
		polar			
DI water	72.8	21.8	25.5	25.5	51.0
ethylene glycol	48.0	29.0	47.0	1.92	19.0
formamide	58.0	39.0	39.6	2.28	19.0
		nonpolar			
diiodomethane	50.8	50.8	0	≈0	≈0
1-bromonaphthalene	44.4	44.4	≈0	≈0	≈0

where γ_S^{LW} is the nonpolar Lifshitz−van der Waals contribution, and γ_S^{AB} is the polar electron-donor/electron-acceptor (Lewis acid−base) component of the energy. Equation 2 states that γ_S^{AB} can be represented in terms of electron-accepting (γ_S^+) and electron-donating (γ_S^-) contributions. Using this approach, the work of adhesion W_A for a liquid/solid system can be expressed as

$$W_A = \gamma_L(1 + \cos\theta) = 2(\sqrt{\gamma_S^{LW}\gamma_L^{LW}} + \sqrt{\gamma_S^-\gamma_L^+} + \sqrt{\gamma_S^+\gamma_L^-}) \quad (3)$$

where the subscripts S and L denote solid and liquid, respectively, and θ is the contact angle.

Equation 3 (the van Oss−Chaudhury−Good equation) provides a simple way to calculate the solid surface free energy from contact-angle measurements using three probe liquids, two of which are polar and one of which is nonpolar. By measuring contact angles for three different liquids and then solving three simultaneous equations, we can calculate the three unknown solid parameters for substitution into eqs 2 and 1. The liquid parameters, γ_L^{LW}, γ_L^-, and γ_L^+, are available from the literature.

The total surface energy γ_S for the azobenzene surface was obtained by solving eqs 1−3. The three components of γ_S were determined using eq 3 from the advancing contact angles of the following probe liquids: water, ethylene glycol, and formamide as polar liquids, and diiodomethane and 1-bromonaphthalene as nonpolar liquids. Table 2 lists the literature values of the total surface energy and components for each probe liquid studied. We used four different combinations of three liquids to estimate the surface energy components. Water was employed in each calculation in order to achieve the largest range of liquid parameters and because of its obvious importance for possible applications. The resulting surface free-energy components are shown in Table 3 and Figure 7. The total surface energy (γ_S)

(26) van Oss, C. J. *Interfacial Forces in Aqueous Media*; Marcel Dekker: New York, 1994.
(27) van Oss, C. J. *Colloids Surf., A* **1993**, *78*, 1.
(28) Weisberg, D. S.; Dworkin, M. *Appl. Environ. Microbiol.* **1983**, *45*, 1338.
(29) van Oss, C. J.; Giese, R. F.; Wu, W. *J. Adhes.* **1997**, *63*, 71.
(30) Jurak, M.; Chibowski, E. *Langmuir* **2006**, *22*, 7226.

Table 3. Surface Free-Energy Components (mJ/m^2) of the ADES-AZO Surface Obtained from Eqs 1−3

liquid combination[a]	illumination	γ_S^{LW}	γ_S^+	γ_S^-	γ_S
a	visible light	32.0	0.0	0.4	32.0
	UV light	38.5	0.0	3.3	39.3
b	visible light	32.0	0.5	1.5	33.6
	UV light	38.5	0.4	5.0	41.3
c	visible light	35.5	0.1	0.3	36.2
	UV light	38.8	0.0	3.3	39.5
d	visible light	35.5	1.0	1.6	38.0
	UV light	38.8	0.4	5.0	41.6

[a] Liquid combinations used for determination of γ_S: (a) DI water, ethylene glycol, diiodomethane; (b) DI water, formamide, diiodomethane; (c) DI water, ethylene glycol, 1-bromonaphthalene; (d) DI water, formamide, 1-bromonaphthalene.

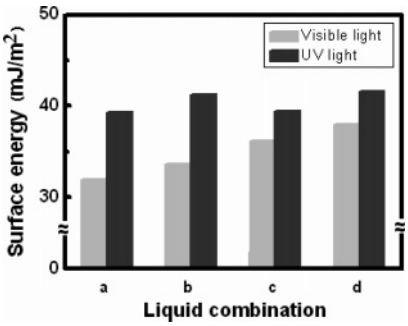

Figure 7. Total surface tension of an ADES-AZO surface after visible and UV irradiation calculated by the LWAB method using the following three-liquid combinations: (a) DI water, ethylene glycol, diiodomethane; (b) DI water, formamide, diiodomethane; (c) DI water, ethylene glycol, 1-bromonaphthalene; and (d) DI water, formamide, 1-bromonaphthalene.

values obtained from different fluid combinations agree reasonably well, given the limitations of the approach. The average total surface energy after UV light exposure (predominantly cis surface) is 40 mJ/m^2, whereas the average value after visible light irradiation (predominantly trans surface) is 35 mJ/m^2. We note that, in this treatment, the trans state of the surface shows the most variation for the different liquid combinations, with the combinations containing the nonpolar probe liquid 1-bromonaphthalene giving higher values than that for the combinations using the nonpolar liquid diiodomethane.

Chemical Nature of the Surface. The van Oss treatment shows that the surface energy is dominated by γ_S^{LW}. The acid and base component contributes on average less than 4% of the total energy. Thus, the interactions of this surface with liquids are mainly via weak induced dipole−induced dipole dispersion interactions, dipole−induced dipole forces, and dipole−dipole forces rather than specific Lewis acid−base or hydrogen bonding interactions. This conclusion is supported by the fact that the average γ_S for the surface enriched in the *trans*-azobenzene (35 mJ/m^2), which has a net dipole moment near zero,[31] is somewhat less than that for the surface enriched in the cis isomer (40 mJ/m^2). Azobenzene in the cis form has a dipole moment of 3.1 D.[31]

Additional information concerning the nature of the interactions between the azobenzene surface and the probe liquids can be gleaned from Figure 6, which shows the advancing contact angle as a function of the liquid surface tension. Liquids that are both hydrogen bond donors and acceptors lie on or above the least-squares lines, while those lacking this property lie on or below the lines. In fact, if the hydrogen-bonding solvents water, ethylene glycol, and formamide are excluded, the slopes of the lines are much less. The contrast is easily seen by comparing ethylene glycol with diiodomethane. Although these have comparable liquid surface tensions, the contact angles for ethylene glycol are ~20° larger than those for diiodomethane. Ethylene glycol (and the other hydrogen bonding solvents) can self-associate via hydrogen-bonding networks, giving a reasonably high surface tension. Hydrogen bonding to the azobenzene surface is much weaker, and the contact angle is thus higher. The energetic cost of spreading on the azobenzene surface is not overcome by attractive interactions with the surface. Diiodomethane molecules, on the other hand, do not hydrogen bond strongly with one another to form extended networks, and this liquid owes its surface tension more to dispersion and dipole−dipole forces. Thus, diiodomethane interacts much more strongly with the azobenzene surface than does ethylene glycol. The free energy is lowered for diiodomethane spreading due to the creation of dipole−dipole and induced-dipole interactions with the azobenzene surface.

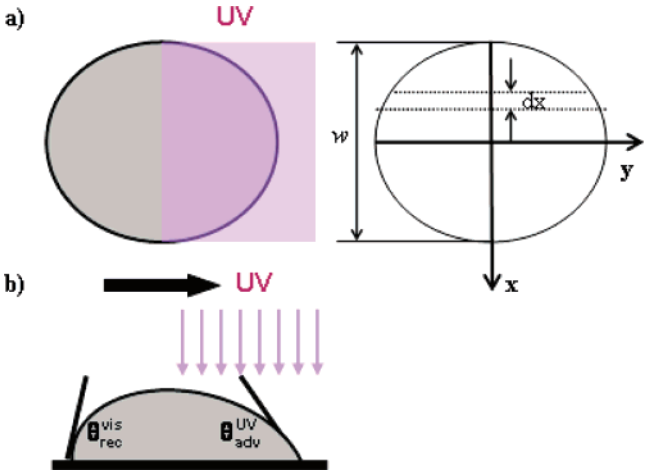

Figure 8. Schematic of UV irradiation on the right side of a droplet and visible irradiation on the left side to induce a gradient in the surface tension, which can lead to light-driven motion in the direction of the arrow on the ADES-AZO substrate: (a) top view; (b) cross section view.

Light-Driven Movement of Liquids. By introducing a sufficiently large spatial gradient in the surface tension across a liquid droplet, the drop can be made to move on a surface. This motion due to a light-induced wettability gradient across the droplet requires that the forces overcome droplet pinning on the smooth surface as characterized by the contact-angle hysteresis, which is the difference between advancing and receding contact angles. Figure 8 illustrates top and cross section views of a liquid drop placed on a surface with one-half of the droplet irradiated with UV light and the other half with visible light to create a spatial gradient in the surface free energy. The unbalanced Young's force for a section of the drop of width dx is given by[11]

$$dF_Y = [(\gamma_{SV} - \gamma_{SL})_{UV} - (\gamma_{SV} - \gamma_{SL})_{vis}]dx \qquad (7)$$

where γ_{SV} and γ_{SL} are the surface free energies of the solid−vapor and solid−liquid interfaces, respectively, after UV or visible irradiation of the surface. If θ_{vis} and θ_{UV} represent the local contact angles at the edges on the two sides of the droplet, then eq 7 can be represented as

$$dF_y = \gamma_{LV}(\cos\theta_{adv} - \cos\theta_{rec})dx \qquad (8)$$

with γ_{LV} being the surface free energy of the liquid−vapor interface. For a drop to move, the force on the drop induced by the gradient in the surface tension represented by the difference

(31) Yager, K. G.; Barrett, C. J. *J. Photochem. Photobiol. A* **2006**, *182*, 250.

in the contact angles must exceed the hysteresis in the contact angles. Specifically, for the drop to be pulled in the direction of the UV irradiation, the advancing angle θ_{adv}^{UV} in the cis state of the ADES-AZO surface must be lower than the receding angle θ_{rec}^{vis} in the trans state. Without considering hydrodynamic forces,[32] the approximate net force F_y on the drop can be expressed by the difference in the advancing and receding contact angles on the two sides of the drop and by integrating eq 8 over the width of the drop, w, giving for the case of Figure 8:

$$F_y = w\gamma_{LV}(\cos\theta_{adv}^{UV} - \cos\theta_{rec}^{vis}) \quad (9)$$

From eq 9, for example, the initial light-induced force on a 1 mm wide benzonitrile droplet irradiated by UV light on one side and visible light on the other would be 2.3 μN based on the measured values for θ_{adv}^{UV} and θ_{rec}^{vis} from Table 1. The force is in the direction of the smaller contact angle.

Thus, for the motion of a liquid drop to be directed by light on a photoswitchable surface, a minimum criterion[11,19] is that the receding contact angle (trans isomer θ_{rec}^{trans}) under visible light must be larger than the advancing contact angle (cis isomer θ_{adv}^{cis}) under UV light. That is, the light-induced contact-angle changes ($\Delta\theta_s = \theta_{adv}^{trans} - \theta_{adv}^{cis}$) should be greater than contact-angle hysteresis in the trans state ($\Delta\theta_h = \theta_{adv}^{trans} - \theta_{rec}^{trans}$). We define the parameter $K = \theta_{rec}^{trans} - \theta_{adv}^{cis} = \Delta\theta_s - \Delta\theta_h$ such that $K > 0$ satisfies this criterion. By spatially controlling the UV/visible irradiation, we anticipate that, for liquids with $K > 0$ on the ADES-AZO surface, it may be possible to move droplets toward the UV light direction.

To test this criterion and identify the liquids that can be moved on the smooth azobenzene-modified surfaces, we measured advancing and receding contact angles before and after UV light irradiation, as was shown in Table 1. We illustrate these results in Figure 9 for the two contrasting cases of a photoinduced switching angle $\Delta\theta_s$ being greater than and less than the hysteresis $\Delta\theta_h$ as defined above for (a) benzonitrile and (b) formamide, respectively. The measured advancing contact angles after visible and UV irradiation for three cycles are shown, and the switching angle and hysteresis (given in Table 1) for the two cases are indicated to the right of the figure. For benzonitrile, $\theta_{rec}^{trans} = 26.2°$, which is greater than $\theta_{adv}^{cis} = 17.0°$, and thus this case fulfills the requirement for motion. As seen in Figure 9, the switching angle for benzonitrile is large compared to the hysteresis, whereas, for formamide, the opposite is the case. Following the above criterion, light-induced motion should be possible for the case of benzonitrile droplets on our ADES-AZO surfaces, but not for the case of formamide droplets.

To investigate the light-guided movement of a droplet of benzonitrile, we placed a 5 μL droplet on the photoresponsive azobenzene-modified surface that had been set to the trans state with visible light, and focused UV light on one edge of the droplet to generate a gradient in the surface photoisomerization. With UV light irradiation, the contact angle of the droplet front edge under UV light irradiation decreased, and the drop spread at the UV-illuminated edge while the back edge of the droplet initially did not move. After 30 s, the droplet undergoes sufficient elongation that the back edge began to move, after which transport of the entire droplet during of the UV irradiation occurred, as

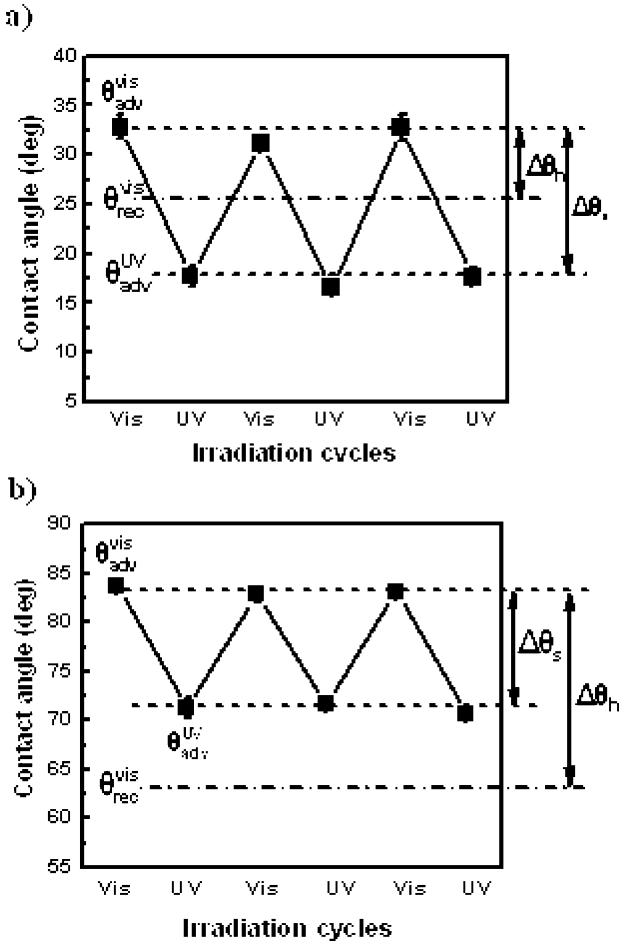

Figure 9. Contact angle of (a) benzonitrile and (b) formamide liquids on an ADES-AZO surface after visible/UV light irradiation. The filled squares (and dashed lines) show the advancing contact angle after visible and UV irradiation, and the dot−dashed line shows the receding contact angle under visible irradiation. $\Delta\theta_h$ is the hysteresis of the ADES-AZO surface after visible irradiation, and is defined as the difference between the advancing and receding contact angles in the trans state. $\Delta\theta_s$ is the switching angle induced by visible/UV light illumination, and is defined as the difference between the advancing contact angles after visible and UV light irradiation. This figure illustrates the criterion that $\Delta\theta_s > \Delta\theta_h$ for a light-induced gradient in surface tension to move droplets, as is found for benzonitrile (a) but not for formamide (b).

predicted from the results of Figure 9a. This shape and position of the droplet during light-driven transport is shown in Figure 10 in a sequence of still photographs taken in side view for the benzonitrile droplet illuminated on the left side with UV light. In contrast, similar irradiation for the case of formamide drops did not result in droplet movement, as expected from Figure 9b.

To further test this criterion we irradiated one side of a 5 μL drop with UV light to test for droplet motion for all the liquids listed in Table 1 on ADES-AZO surfaces that had been set to the trans state with visible light while imaging the drops in side view. A summary of the photoinduced switching angle and the hysteresis for all the liquids studied along with the results for drop movement is given in Figure 11, where "y" indicates that the droplet moves, and "n" means that it remains pinned. Benzonitrile, 1-bromonaphthalene, DMF, and 1-methylnaphthalene fulfill the requirement of $K > 0$ and were all found to move by spatial irradiation of one side of the drop with UV light. Likewise, DI water, formamide, and ethylene glycol, for which $K < 0$, did not move. For 1-methylnaphthalene, which had the

(32) Shankar, R. S.; Moumen, N.; McLaughlin, J. B. *Langmuir* **2005**, *21*, 11844.
(33) Reichardt, C. *Solvents and Solvent Effects in Organic Chemistry*, 2nd ed.; Basel: Weinheim, Germany, 1988.
(34) Abboud, J.-L. M.; Notario, R. *Pure Appl. Chem.* **1999**, *71*, 645.
(35) Kalugin, O. N.; Lebed, A. V., Vyunnik, I. N. *J. Chem. Soc. Faraday Trans.* **1998**, *94*, 2103.

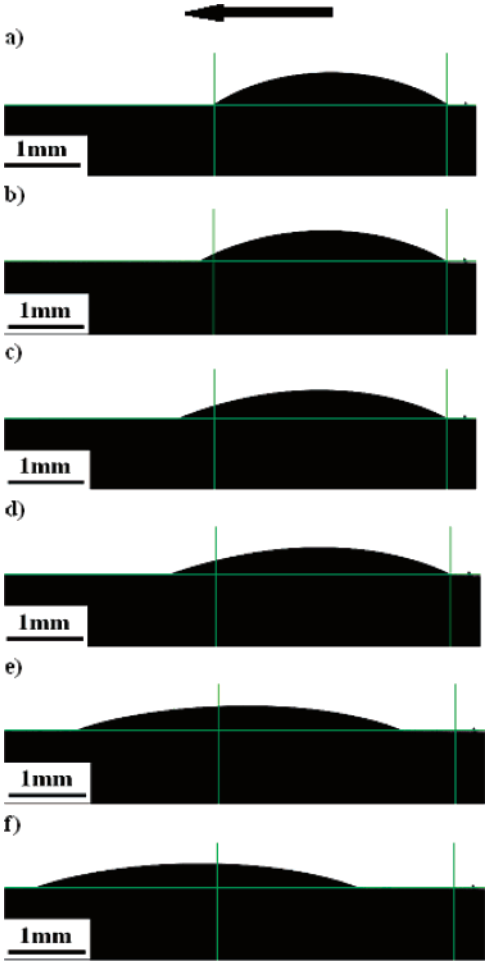

Figure 10. Time sequence of side view photographs (a−f) of a benzonitrile droplet on an ADES-AZO surface, illustrating light-driven transport by UV light. The UV illumination is on the left edge of the droplet, and the droplet is shown in a series of still frames as it moves to the left.

smallest positive *K* value (0.2°), droplets moved relatively small distances before becoming pinned, presumably because of some nonuniformities on the surface. Also, for the case of diiodomethane, which had a very small but positive *K* value (1.6°), droplet motion was not consistently achieved. Measurements were not carried out for acetonitrile because of the rapid evaporation of the drop due to its high vapor pressure. Summarizing our results, it was possible to achieve light-induced motion of drops for liquids that had measured $K > 0$, whereas all liquids with $K < 0$ were pinned. Additional images of the motion of droplets for 1-bromonaphthalene and DMF along with a tabulation of our measured *K* values are shown in the Supporting Information as Table 2.

Several correlations were explored between the strength of the driving force for moving liquid droplets with light gradients and the solvent parameters for the liquids studied here. While, as anticipated for the complex case of a surface tension gradient inducing droplet motion, no strong correlations were observed, there were several trends. As shown in Figure 12a, liquids with lower values of surface tension tend to be easier to move. This is consistent with the generally lower hysteresis in the contact angle in the trans state also found here for liquids with lower surface tensions (see Table 1 and the Supporting Information), and indicative that drops are more easily moved on a surface when less energy is required to overcome the liquid surface tension. Also, as shown in Figure 12b, the magnitude of the

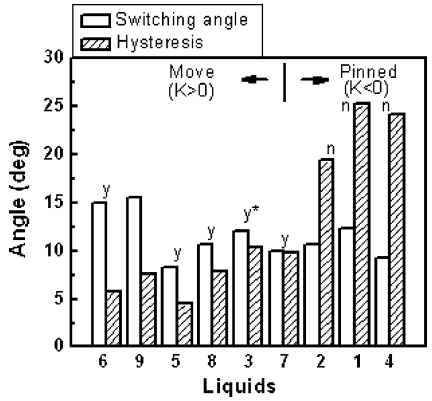

Figure 11. UV−visible contact-angle switching $\Delta\theta_s$ and the contact-angle hysteresis θ_h under visible light measured for different liquids on the ADES-AZO surface. Those liquids that were found to move under UV light irradiation on one side are labeled "y", and those that did not are labeled "n". The liquids are ordered from left to right in decreasing *K* ($K = \Delta\theta_s - \Delta\theta_h$) value where droplet motion is expected for $K > 0$. The liquids as numbered on the *x* axis are (1) DI water, (2) formamide, (3) diiodomethane, (4) ethylene glycol, (5) 1-bromonaphthalene, (6) benzonitrile, (7) 1-methylnaphthalene, (8) DMF, and (9) acetonitrile. For diiodomethane (marked by an asterisk), the droplet could not be consistently moved. Droplet motion was not measured for acetonitrile because of the rapid evaporation of this high vapor pressure liquid.

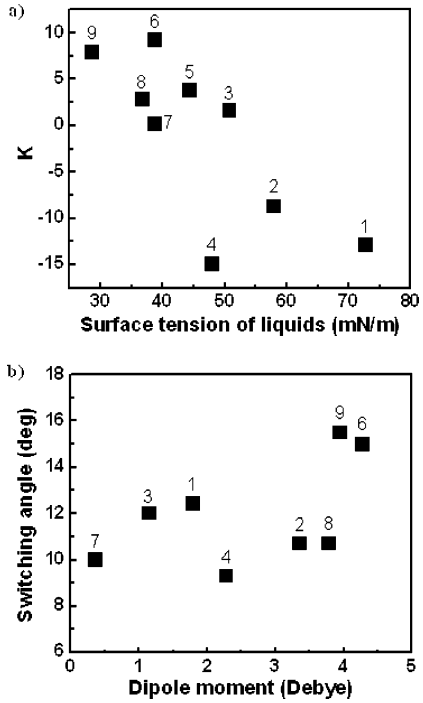

Figure 12. (a) *K* parameter values obtained from contact-angle measurements on the azobenzene-functionalized surface vs the surface tension of the probe liquids. Positive *K* values are required to satisfy the criterion for droplet motion. (b) Switching angle for UV−visible irradiation of the probed liquids as a function of their dipole moment on the azobenzene-functionalized surface. Liquids are (1) DI water,[33] (2) formamide,[33] (3) diiodomethane,[34] (4) ethylene glycol,[35] (6) benzonitrile,[34] (7) 1-methylnaphthalene,[34] (8) DMF,[34] and (9) acetonitrile.[34]

optically induced switching angle tends to increase with the dipole moment of the liquid. This switching of the contact angle provides the driving force needed to overcome the hysteresis and move droplets on a photochromic surface. The liquids ethylene glycol, formamide, and DMF appear as exceptions to this trend, pointing to the importance of the dipole−dipole interactions between the

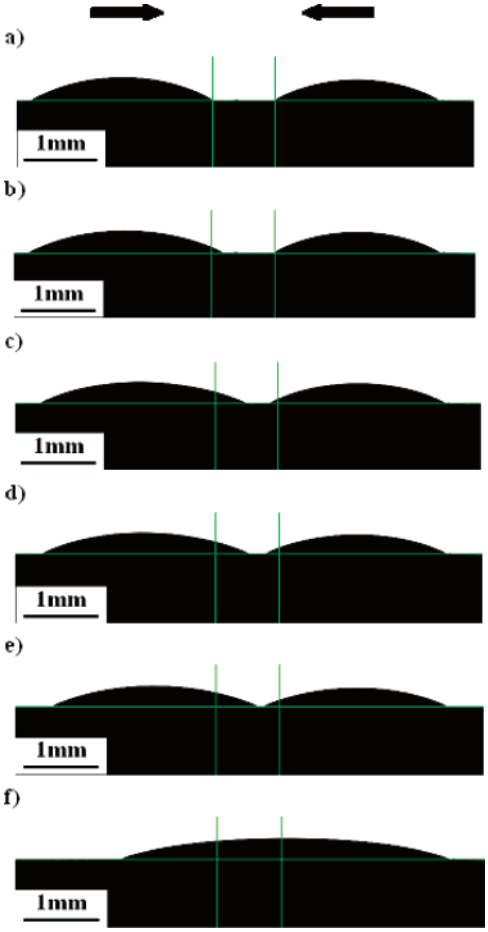

Figure 13. Time sequence of side-view photographs (a−f) showing UV light driving two droplets of benzonitrile on an ADES-AZO surface to move toward each other and combine. The UV illumination is in the middle, extending to the two interior edges of the droplets.

solvent liquid and azobenzene moiety relative to any hydrogen-bond-forming interactions, since the azobenzene undergoes a dramatic change in dipole moment from approximately 0 to 3 D upon switching from trans to cis states.

To further illustrate the potential for droplet control in microfluidics, we demonstrated the optically controlled combining of droplets for benzonitrile. In Figure 13 two drops of benzonitrile are shown in a series of still images for which UV light simultaneously irradiated the region between and at the edges of two drops. The UV light irradiation resulted in the droplets moving together and mixing within 1 min. Light-driven liquid motion thus provides an alternative nonmechanical method to manipulate small volumes of liquids on surfaces without containers or channels.

3. Conclusions

The present work demonstrates the use of a light-induced gradient in the surface tension to move liquids on smooth surfaces functionalized with a photoresponsive monolayer. A synthetic surface modification approach was developed to functionalize substrates with a photochromic azobenzene derivative, which exhibited large and reversible changes in wetting angle after UV and visible light irradiation. The dynamic advancing and receding contact angles of droplets on this surface were measured for a variety of liquids for the surface optically switched into the cis and trans states. The surface free energy of these azobenzene-modified surfaces in the two optically switched states was characterized by the van Oss theory. Liquid droplet motion in the direction of the UV light was achieved by irradiation with a UV−visible optical gradient across the drop. The driving force for the optically directed motion of liquids was related to the measured advancing and receding contact angles, and the motion of liquid droplets on the photochromic surface was demonstrated and characterized for a variety of liquids. Good agreement was achieved in comparisons to a contact-angle criterion for moving droplets and the observation of droplet motion. These results provide additional understanding of the ability to control droplet motion with light for various solvents and have potential applicability to microfluidic systems for delivering analyses in lab-on-a-chip environments.

Acknowledgment. This work was supported in part by the U.S. Department of Energy, Sandia National Laboratories (Contract DE-AC04-94AL85000) and the Center for Nanotechnologies at Los Alamos National Laboratory (Contract W-7405-ENG-36), and the National Science Foundation (DMR-0413523 and CHE-0352599). Support was also provided by the Interdisciplinary Network of Emerging Science and Technology (INEST).

Supporting Information Available: The error values for the dynamic advancing and receding contact angles, the measured *K* values, and still photographs illustrating light-induced motion for 1-bromonaphthalene and DMF. This information is available free of charge via the Internet at http://pubs.acs.org.

LA701507R